



CHALMERS
UNIVERSITY OF TECHNOLOGY

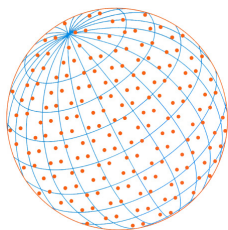
Trends in Air Pollution in Europe, 2000–2019

Downloaded from: <https://research.chalmers.se>, 2025-12-04 23:27 UTC

Citation for the original published paper (version of record):

Aas, W., Fagerli, H., Alastuey, A. et al (2024). Trends in Air Pollution in Europe, 2000–2019. *Aerosol and Air Quality Research*, 24(4). <http://dx.doi.org/10.4209/aaqr.230237>

N.B. When citing this work, cite the original published paper.



Special Issue:

Carbonaceous Aerosols in the
Atmosphere (I)

OPEN ACCESS 

Received: October 1, 2023

Revised: February 2, 2024

Accepted: February 4, 2024

*** Corresponding Author:**

waa@nilu.no

Publisher:

Taiwan Association for Aerosol
Research

ISSN: 1680-8584 print

ISSN: 2071-1409 online

 **Copyright:** The Author(s).

This is an open access-article
distributed under the terms of the
[Creative Commons Attribution
License \(CC BY 4.0\)](https://creativecommons.org/licenses/by/4.0/), which permits
unrestricted use, distribution, and
reproduction in any medium,
provided the original author and
source are cited.

Trends in Air Pollution in Europe, 2000–2019

Wenche Aas ^{1*}, Hilde Fagerli ², Andres Alastuey ³, Fabrizia Cavalli⁴,
Anna Degorska ⁵, Stefan FeigenSPAN⁶, Hans Brenna ², Jonas Gliß ²,
Daniel Heinesen ², Christoph Hueglin ⁷, Adéla Holubová ⁸,
Jean-Luc Jaffrezo ⁹, Augustin Mortier ², Marijana Murovec¹⁰,
Jean-Philippe Putaud ⁴, Julian Rüdiger ⁶, David Simpson ^{2,11},
Sverre Solberg ¹, Svetlana Tsyro ², Kjetil Tørseth ¹, Karl Espen Yttri ¹

¹ NILU, EMEP/CCC Kjeller, Norway

² Norwegian Meteorological Institute, EMEP/MSC-W, Oslo, Norway

³ Institute of Environmental Assessment and Water Research, Barcelona, Spain

⁴ European Commission, Joint Research Centre, Ispra (VA), Italy

⁵ Institute of Environmental Protection, National Research Institute, Warsaw, Poland

⁶ The Umweltbundesamt (UBA), Dessau-Roßlau, Germany

⁷ EMPA, Swiss Federal Laboratories for Materials Science and Technology, Dübendorf, Switzerland

⁸ Czech Hydrometeorological Institute, Košice, Czech Republic

⁹ Institut des Géosciences de l'Environnement, Université Grenoble Alpes, CNRS, IRD, Grenoble
INP, Grenoble, France

¹⁰ Slovenian Environment Agency, Ljubljana, Slovenia

¹¹ Department of Space, Earth and Environment, Chalmers University of Technology, Sweden

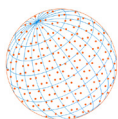
ABSTRACT

This paper encompasses an assessment of air pollution trends in rural environments in Europe over the 2000–2019 period, benefiting from extensive long-term observational data from the EMEP monitoring network and EMEP MSC-W model computations. The trends in pollutant concentrations align with the decreasing emission patterns observed throughout Europe. Annual average concentrations of sulfur dioxide, particulate sulfate, and sulfur wet deposition have shown consistent declines of 3–4% annually since 2000. Similarly, oxidized nitrogen species have markedly decreased across Europe, with an annual reduction of 1.5–2% in nitrogen dioxide concentrations, total nitrate in the air, and oxidized nitrogen deposition. Notably, emission reductions and model predictions appear to slightly surpass the observed declines in sulfur and oxidized nitrogen, indicating a potential overestimation of reported emission reductions. Ammonia emissions have decreased less compared to other pollutants since 2000. Significant reductions in particulate ammonium have however, been achieved due to the impact of reductions in SO_x and NO_x emissions. For ground level ozone, both the observed and modelled peak levels in summer show declining trends, although the observed decline is smaller than modelled. There have been substantial annual reductions of 1.8% and 2.4% in the concentrations of PM₁₀ and PM_{2.5}, respectively. Elemental carbon has seen a reduction of approximately 4.5% per year since 2000. A similar reduction for organic carbon is only seen in winter when primary anthropogenic sources dominate. The observed improvements in European air quality emphasize the importance of comprehensive legislations to mitigate emissions.

Keywords: Transboundary, Air pollution, Compliance monitoring, Aerosols, Deposition

1 INTRODUCTION

Under the United Nations Economic Commission for Europe (UNECE) Convention on Long-range Transboundary Air Pollution (CLRTAP) there are several legally binding protocols. The latest one



is the 2012 amended Gothenburg Protocol, which abates acidification, eutrophication and ground level ozone (UNECE, 2012). The Protocol entered into force in October 2019, and this initiated a review to assess the progress made towards achieving the environmental and health objectives of the Protocol. The amended Protocol includes legally binding emission reduction commitments for 2020 for the major air pollutants: sulfur dioxide (SO₂), nitrogen oxides (NO_x), ammonia (NH₃), volatile organic compounds (VOCs), and fine particulate matter (PM_{2.5}).

The cooperative programme for monitoring and evaluation of long-range transmission of air pollutants in Europe (EMEP) is an integral component of LRTAP, and it relies on three main elements: (1) collection of emission data, (2) measurements of air and precipitation quality data and (3) modelling of atmospheric transport and deposition of air pollution. Through the combination of these three elements, the quantity and significance of transboundary fluxes and related exceedances to critical loads and threshold levels can be assessed. The EMEP model results are an essential input to integrated assessment models and to a number of Protocols and the European Union National Emission Ceilings Directive. It is critical that the model responds correctly to emission changes to give confidence in its ability to predict concentrations and depositions for present and future emission scenarios. The response of a model to emission and deposition changes can be assessed by comparison to long-term observational data. In this paper we present an assessment of the trends in air pollution in Europe for the period 2000–2019, based on observational data from the EMEP network, as well as EMEP MSC-W model calculations. We analyzed trends in air concentrations for ozone, sulfur dioxide, particulate matter (and their components sulfate, nitrate, ammonium, elemental- and organic carbon), as well as oxidized and reduced nitrogen, along with wet deposition of sulfur and nitrogen species. For elemental- and organic carbon (EC/OC), we present trends for the 2010–2019 period due to lack of longer observed timeseries for these components.

Unfortunately, the EMEP observational network is dominated by sites in the western parts of the EMEP domain and has hardly any coverage in the EECCA (Eastern Europe, Caucasus and Central Asia) countries. Therefore, the assessment discussed here is only valid for a part of the EMEP domain (EU27 + UK + EFTA countries).

There have been several studies of sulfur, nitrogen, PM and ozone trends in Europe throughout the forty years of the EMEP programme (Banzhaf *et al.*, 2015; Colette *et al.*, 2016, 2021; Fagerli and Aas, 2008; Jonson *et al.*, 2006; Simpson *et al.*, 2022; Theobald *et al.*, 2019; Tørseth *et al.*, 2012; Tsyro *et al.*, 2022; Vivanco *et al.*, 2018). However, this is to our knowledge, the first comprehensive European overview of trends in observations and model results in carbonaceous aerosols. This enables a better assessment of changes in the chemical composition in PM₁₀ and PM_{2.5}.

It should also be pointed out that for the different components analyzed, the number of observational sites available and the geographical coverage differ.

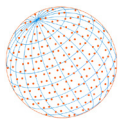
2 METHODOLOGY

2.1 Setup for EMEP MSC-W Model Calculations

The EMEP MSC-W model version rv4.42 (Simpson *et al.*, 2012, 2021) has been used to perform model runs for years from 2000 through 2019. The horizontal resolution is 0.1° × 0.1° with 20 vertical layers (the lowest with a height of approximately 50 meters). Meteorology, emissions, boundary conditions and forest fires for the respective years have been used as input. Meteorological data have been derived from ECMWF-IFS (cy40r1) simulations for the years 2000 to 2018 and from an ECMWF-IFS (cy46r1) simulation for 2019. The boundary conditions for the main gaseous and aerosol species were based on climatological observed values with prescribed trends in trans-Atlantic fluxes, while the ozone boundary levels have been based on measurements of ozone in incoming westerly air masses at Mace Head in Ireland (Simpson *et al.*, 2012).

The anthropogenic emission input data are based as far as possible upon emissions per sector and grid square officially reported to CLTRAP, available in 2021 (EMEP, 2021).

The speciation of PM emissions into emissions of elemental carbon (EC), primary organic aerosol (POA), and remaining primary particle matter (remPPM) components was based on ECLIPSE v6b emission data (Klimont *et al.*, 2017). The condensable component of particulate matter is a class



of organic compounds of low volatility that may exist in equilibrium between the gas and particle phase. It is probably the biggest single source of uncertainty in PM emissions (Denier van der Gon *et al.*, 2015; Simpson *et al.*, 2020, 2022).

2.2 Observations

The observations used have all been reported to EMEP and are openly available from the EBAS database (<http://ebas.nilu.no>). For EC and OC, only observations using the reference method EUSAAR-2 (Cavalli *et al.*, 2010) have been selected and, due to the lack of a long consistent time series, statistics have only been compiled for these compounds in the last decade. Further, visual inspection of the time series revealed some data sets with very high annual variability and inconsistency in the time series, like sudden drops or increase. This can be due to contamination of the samples, a change in methods, or the influence of local sources from the surrounding areas. Some of these timeseries have been excluded. Data from sites which have been moved a very short distance during the period have been combined into one timeseries. Further, sites not representative when comparing with a model of $0.1^\circ \times 0.1^\circ$ resolution (for example mountain top sites) have been excluded. An overview of the in total 146 sites that have been used for the different components and periods are found in Table S1 in the Supplementary. It should be remembered that all the EMEP sites are in rural areas away from cities and therefore representing the European rural background. The analytical methods used are described in the annual EMEP data reports (Hjellbrekke, 2021; Hjellbrekke and Solberg, 2021).

2.3 Method for Calculation of Trends

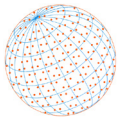
Trends for the sulfur and nitrogen compounds, EC/OC, PM, and ozone were computed based on yearly averages of the original daily data with a criterion of at least 75% data coverage each year. For seasonal averages, at least one monthly value was required with 75% data coverage. A data capture requirement of ca 75% was also applied for yearly averages, i.e., requiring at least 14 yearly values for the period 2000–2019.

For O₃, a different approach for the data aggregation was applied. Firstly, daily maximum concentrations were computed based on hourly measurements, requiring at least 18 hourly measurements per day corresponding to a 75% data capture as for the other variables. Subsequently, annual percentiles were computed based on the daily maximum values, requiring at least 90% valid daily data, corresponding to 330 daily values. The reason for this strict criterion is that the high ozone episodes typically cover a short period of the year. Trends were then calculated for several annual percentiles.

The same methodologies as described in earlier studies (Aas *et al.*, 2019; Mortier *et al.*, 2020) have been used to calculate the trends in both model and observational data at all the individual sites. The significance of the trends is tested with the Mann-Kendall test (Hamed and Ramachandra Rao, 1998). The related *p*-value is used to determine if the trend is significant or not. A *p*-value less than 0.05 is defined as statistically significant. The slope is calculated with the Theil-Sen estimator which is less sensitive to outliers than standard least-squares methods (Sen, 1968). The trend is provided as a relative trend (% yr⁻¹) with respect to the first year of the time-period, i.e., the intercept of the Sen's slope. The trends presented are calculated by taking the averages of the Sen slopes or the relative trends for all the sites, including those with non-significant trends. In addition, confidence intervals for these mean values were calculated. It should be noted that these 95% confidence intervals for the average trends will be less accurate when the number of sites with significant trends is low.

3 RESULTS AND DISCUSSION

Both observed and modelled trends spanning the years 2000–2019 were computed. For most compounds, the reported emissions do not follow a linear trend over the whole period, but typically flattens out in the last years. To assess if there are differences in the observed and modelled trends between the two decades, decadal trends for 2000–2010 and 2010–2019 were analysed separately. Additionally, the period 2005–2019 was included, aligning with 2005 as the base year of the



Gothenburg Protocol. The statistics of absolute and relative average changes for all the periods and seasons are found in Supplementary Tables S3–S21.

3.1 Trends of Sulfur Compounds

Emissions of SO_2 have declined by more than 80% ($-4.3\% \text{ yr}^{-1}$) within the area of the EU27 + UK + EFTA countries the last two decades (Table S2). Both the observed and modelled trends for all the atmospheric sulfur components show substantial decreases (Fig. 1) in line with previous trend studies (Aas *et al.*, 2019; Theobald *et al.*, 2019; Vivanco *et al.*, 2018). Most of the time series show significant trends for the 20-year period for all considered compounds (Tables S3–S5).

The spatial distribution of the relative trends (Fig. 2) shows that the decreases in sulfur air concentrations and wet deposition have been quite homogeneous across Europe (west of Russia), though somewhat higher in Spain and France and lower in Poland. Both model and observations show higher reductions in the primary component SO_2 compared to secondary SO_4^{2-} . The greater decrease in SO_2 compared to secondary sulfate is likely due to a combined effect of higher oxidation rate (hence more SO_2 converted to SO_4^{2-}) and increased dry deposition rate of SO_2 . One possible explanation is that the oxidation capacity of the atmosphere may have increased as the emissions have decreased (Dalsøren *et al.*, 2016). This would give less acidic clouds due to less SO_2 and only slight decreases in NH_3 which has increased the oxidation rate of SO_2 to SO_4^{2-} via the ozone pathway (Banzhaf *et al.*, 2015; Redington *et al.*, 2009). In addition, less acidity in the environment probably leads to more efficient dry deposition of SO_2 (Fowler *et al.*, 2009).

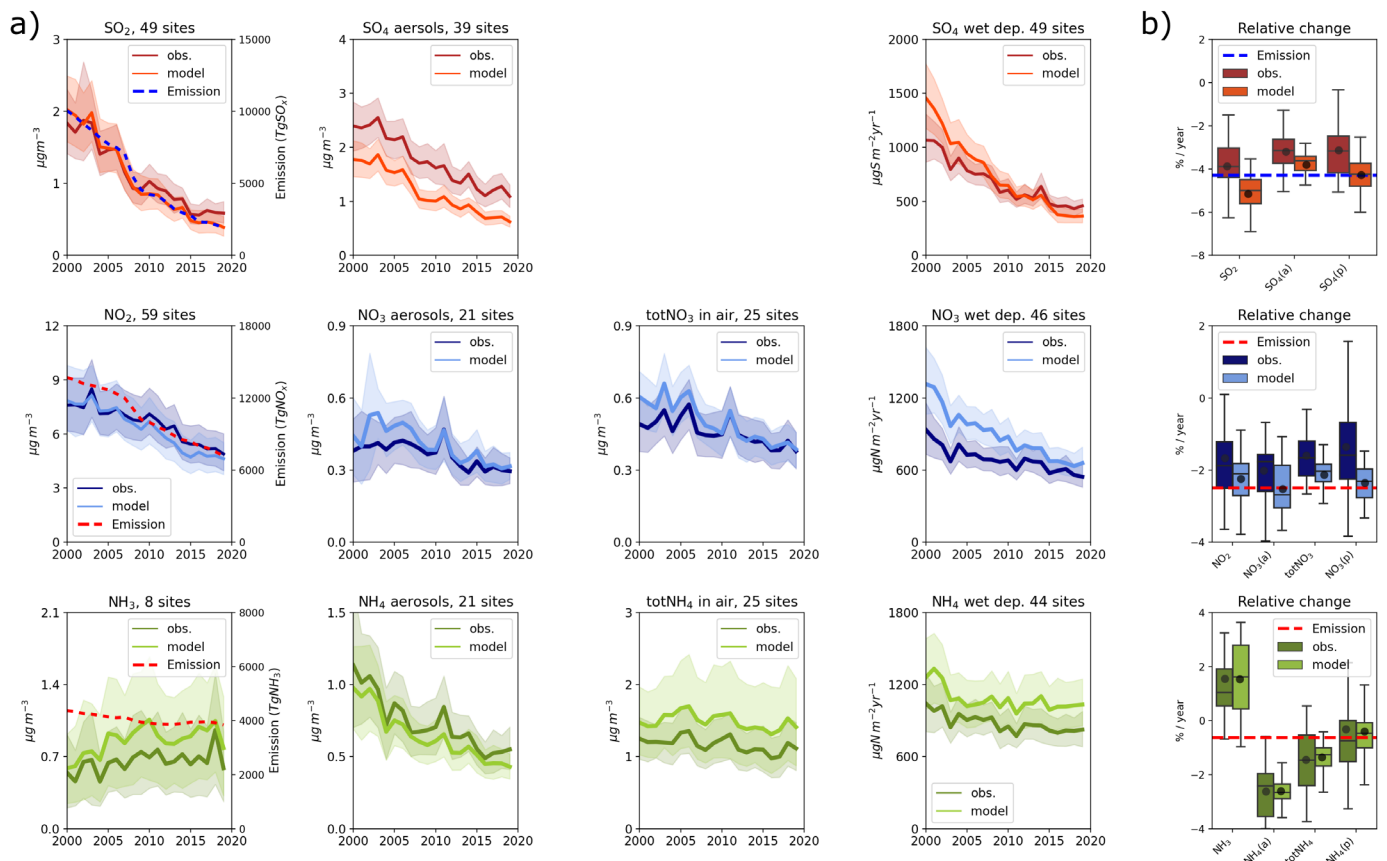


Fig. 1. Trends in sulfur and nitrogen components from 2000–2019 for EMEP observations and model, compared to the emission trends. The solid line in the time series plots (a) indicate the average annual mean concentrations for all the sites and the shaded area the 95% confidence interval. The box plots (b) represent the 50th, 25th, and 75th percentiles and the whiskers lie within the 1.5 inter-quartile ranges for the trends of all the sites, including those with not significant trends. In addition, the mean trends are indicated with black circles.

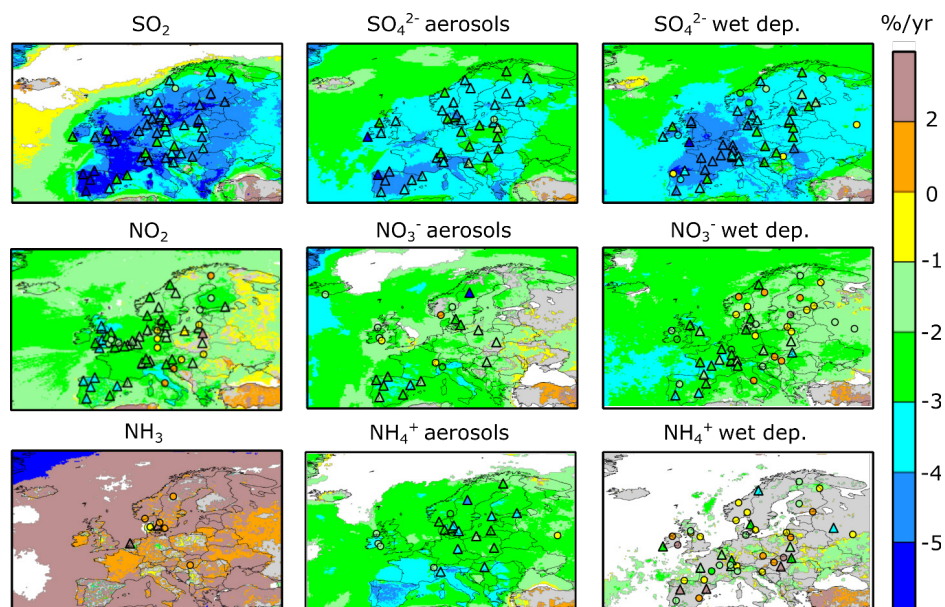
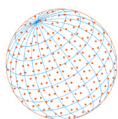


Fig. 2. Relative trends in sulfur and nitrogen components from 2000–2019: EMEP modelled are shown as coloured contours (grey/white means non-significant trends) and observed by coloured triangles (significant) and circles (non-significant).

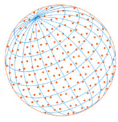
The average observed trends for the last 20 years (2000–2019) are -3.9 ± 0.3 , -3.2 ± 0.3 , and $-3.1 \pm 0.3\% \text{ yr}^{-1}$ for SO_2 , SO_4^{2-} in aerosols and SO_4^{2-} in wet deposition, respectively, while the trends in model calculations are somewhat greater: -5.1 ± 0.3 , -3.8 ± 0.2 , and $-4.3 \pm 0.2\% \text{ yr}^{-1}$, respectively. The model exhibits an overestimation of the declining sulfur trends, seen both in the relative and absolute trends for SO_2 and wet deposition of SO_4^{2-} , while for SO_4^{2-} in aerosols the absolute reductions in concentrations is higher in observations, but within the 95% confidence interval of the modelled trends (Table S3).

It is not clear why the trends calculated by the model are larger than the trends in observations. The mismatch between the calculated trends and the observed trends are particularly large for eastern Spain and parts of eastern Europe (Fig. 2). Assuming that the observations are representative for the area, these differences indicate that the emission reductions reported by some countries are probably somewhat optimistic. However, firm conclusions are difficult to draw as we do not monitor the full sulfur budget (e.g., dry deposition of sulfur is lacking). Furthermore, changes in the spatial distribution of the emissions may not be correctly accounted for and missing processes in the model could also play a role.

There are not large differences in the relative trends between seasons, and the differences in the relative trends between the two decades are small. The reductions in sulfur oxide (SO_x) emissions are 58% for 2000–2010 and 55% for 2010–2019 (Table S2), and in the observations the total changes in these two periods are between 26–43% for all the different sulfur compounds in 2010–2019 and 25–44% for 2000–2010. For the model estimates the reductions are between 38–50% and 42–54%, respectively.

3.2 Trends in Oxidised Nitrogen

Over the last few decades, there has been a significant decline in the emissions of NO_x in Europe, a total reduction of 48% ($2.5\% \text{ yr}^{-1}$) since 2000 (Table S2). This decline has resulted in reduced concentrations of NO_2 , total nitrate (comprising nitric acid and particulate nitrate) in air, and oxidized nitrogen wet deposition at EMEP background sites (Fig. 1). EMEP MSC-W model calculations follow the reported emission reductions closely with a total reduction of $43 \pm 3\%$ ($2.2 \pm 0.2\% \text{ yr}^{-1}$). However, the reductions of observed NO_2 concentrations are lower than the reported emission and the modelled ones, with an average of $1.7 \pm 0.4\% \text{ yr}^{-1}$ or in total $32 \pm 7\%$ for the 2000–2019 period. Notably, the observed trends vary more between sites than the modelled,



and the median of the observed and modelled trends are somewhat closer, $-1.9\% \text{ yr}^{-1}$ and $-2.1\% \text{ yr}^{-1}$, respectively (Fig. 1).

The trends derived from observations, model and emissions agree well for the last period (2010–2019), with trends around $-2.7\% \text{ yr}^{-1}$ whilst the trend in the first period is substantially lower in the observations than in the model calculations and emissions. From Fig. 1, the agreement in average concentrations between observations and model calculations is excellent until around 2008, but from 2009 on the model (and emissions) is shifted down relative to the observations. Similar results have been found in Colette *et al.* (2021) using data both from Airbase and EMEP. As NO_2 has a short lifetime (a few hours to days), the trend in NO_2 is expected to reflect the trend in (local) emissions of NO_x ; thus, the comparison between average European emission trends may not reflect more local changes in emissions. However, these findings indicate that the reported European emissions have most probably been too optimistic, which is also seen in other studies (Jiang *et al.*, 2022; Vaughan *et al.*, 2016; Oikonomakis *et al.*, 2018). Jiang *et al.* (2022) found large uncertainties in the trends of anthropogenic nitrogen oxides (NO_x) emissions over Europe (15–45% in 2005–2018) when using different methods to quantify the trend. They suggest that the shift of the largest NO_x sources being power generation to industry and transport have caused smaller effects of emission controls and find that in general the official emission inventories (as used in this study) show lower reductions than the science-based inventories. Vaughan *et al.* (2016) suggest that NO_x emissions from traffic is underestimated compared to real world road traffic emissions.

The trends in wet deposition of oxidized nitrogen reflect changes in long-range transported oxidized nitrogen (e.g., NO_x has been converted to nitric acid and particulate nitrate and then washed out by rain) and are less sensitive to local changes. The trends for wet deposition of nitrate are also lower in the observations than in the model calculations (and emissions of NO_x) for the 2000–2019 period. Whilst the average of the trends in observations is $-1.4 \pm 0.4\% \text{ yr}^{-1}$ (total of $-26 \pm 7\%$), the model calculates the trend at the same sites to be $-2.4 \pm 0.1\% \text{ yr}^{-1}$ (total of $-45 \pm 3\%$), close to the trends in emissions from the western EMEP domain (-48%).

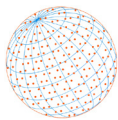
For particulate nitrate, nitric acid and their sum, the results are more complex. The number of sites is small (especially for nitric acid, with only 6 sites), the coverage of Europe more scattered, and the gas/aerosol partitioning to nitrate and nitric acid is methodologically biased (Aas *et al.*, 2012).

The modelled trends of particulate nitrate, nitric acid, and their sum for 2000 to 2019 are all around -2 to $-2.5\% \text{ yr}^{-1}$ and thus aligned with the results for NO_2 , wet deposition of oxidized nitrogen and the emissions of NO_x . The observations show a somewhat smaller negative trend, $1.6 \pm 0.4\% \text{ yr}^{-1}$ for the sum, and around $2\% \text{ yr}^{-1}$ both for particulate nitrate and nitric acid. For the shorter periods, the number of sites with significant trends are very small, both in the model calculations and the observations, and thus the results are more uncertain.

The relative trends for NO_2 and wet deposition of oxidized nitrogen for observations from the eastern EMEP domain are smaller and to a larger extent non-significant, whilst the trends in model calculations are in general larger and more often significant (Fig. 2). The reasons for these discrepancies are not clear but could be related to problems/inaccuracies in emission reporting and their trends, all the processes may not be defined well enough, and there might be biases in the observations.

3.3 Trends in Reduced Nitrogen

Ammonia emissions from agricultural activities have only been slightly reduced (-12%) for the western EMEP domain since 2000 (Table S2). In the EMEP domain as a whole, ammonia emissions have increased by 12% since 2000 (EMEP, 2021). With such small changes in emissions, it is very difficult to detect any trends in the observations, considering also that the meteorological variability introduces year-to-year changes of the same magnitude as the expected trends. This is reflected in both observations and model calculations where we find very few significant trends in wet deposition of reduced nitrogen. Out of 44 sites with long term measurements of wet deposition, only 13 are significant for the observations and 9 for the model (Table S14). The average change in the observations for 2000 to 2019 is $-0.3 \pm 0.7\% \text{ yr}^{-1}$ while the model shows an average trend of $-0.4 \pm 0.3\% \text{ yr}^{-1}$ (Fig. 1). For the shorter time periods there are even fewer sites with significant



trends (see details in Supplementary Tables). Note that previous studies (Theobald *et al.*, 2019; Tørseth *et al.*, 2012) have found decreasing trends for reduced nitrogen. However, those studies analysed earlier periods (e.g., 1980–2009 or 1990–2009), where the reported ammonia emissions decreased more.

Total ammonium ($\text{NH}_3 + \text{NH}_4^+$) in air shows larger changes in observations of about $-1.5 \pm 0.5\% \text{ yr}^{-1}$ ($-28 \pm 10\%$ totally for the period) compared to the model with $-1.4 \pm 0.2\% \text{ yr}^{-1}$ ($-26 \pm 4\%$), and with a larger fraction of the sites having significant trends. This trend is larger than the reduction in ammonia emissions for EU27 + UK + EFTA countries (-12%). The trend for ammonium aerosols is even more negative, $-2.6 \pm 0.4\% \text{ yr}^{-1}$, similar in observations and model calculations. Very few sites have long-term timeseries of ammonia in air (8 sites), and very few of the trends calculated are significant. However, on average, the changes observed and calculated are positive: $+1.5\% \text{ yr}^{-1}$ with all values within the confidence interval being positive (Table S12).

This large difference between the trends of the different reduced nitrogen components (Fig. 1 and Fig. 2) can be explained by the interaction of ammonia with the sulfur and nitrogen components. When ammonia is released into the air, it reacts with sulfuric acid originating from SO_2 oxidation and forms particulate ammonium sulfate. During the years from 2000 onwards, large reductions in SO_x and NO_x emissions have taken place, and thus less sulfuric acid and nitric acid is available for forming ammonium particles. Therefore, a smaller fraction of NH_3 is converted to aerosol ammonium, and the decrease in particulate ammonium is strongly linked to the decrease in sulfate and nitrate (Grange *et al.*, 2023). It is therefore to be expected that the trend in ammonium aerosol ($-2.6 \pm 0.4\% \text{ yr}^{-1}$, observations) lies somewhere between the trend in particulate sulfate ($-3.2 \pm 0.3\% \text{ yr}^{-1}$, observations) and nitrate ($-2.0 \pm 0.5\% \text{ yr}^{-1}$, observations).

When less ammonia is converted to ammonium, the (very small) decrease in ammonia emissions is compensated by a larger part of ammonia residing in the gas phase, and no decreases in ammonia (very few significant trends) are detected. For the sum of ammonia and ammonium, the two opposite trends of ammonia (no trend or slightly positive) and ammonium (negative) results in a negative trend that is smaller than the trend for ammonium alone.

The analysis done for the shorter periods (Tables S11–S14) confirms the explanations discussed above. It is worth noting that the agreement between the trends obtained from model and observation data is excellent for the different reduced nitrogen components, which indicates that the EMEP MSC-W model does a reasonably good job in reproducing the non-linear interactions between sulfur, oxidized nitrogen and reduced nitrogen and how this has evolved during the past 20 years.

3.4 Trends in Elemental and Organic Carbon

Elemental and organic carbon (EC/OC) has not been part of the EMEP monitoring programme as long as the species regulated in the Gothenburg protocol, thus, to assess the trends in these compounds, we only look at the last ten years period (2010–2019).

The average observed trends in EC for 2010–2019 for 15 sites shows a reduction of $4.5 \pm 1.5\% \text{ yr}^{-1}$ (Fig. 3). This is comparable to the reduction ($-5.0 \pm 0.9\% \text{ yr}^{-1}$) calculated for the eleven sites where the reduction was statistically significant. The reduction was rather similar considering only these eleven sites, ranging from $-4.2\% \text{ yr}^{-1}$ to $-5.8\% \text{ yr}^{-1}$ for ten out of eleven sites. The largest reduction was seen amongst the sites with the highest EC levels, i.e., at Iskrba ($-7\% \text{ yr}^{-1}$) in Slovenia and at Ispra ($-5.8\% \text{ yr}^{-1}$) in the Po Valley region in Northern Italy (Fig. 3). Notably, these were the only sites where a statistically significant reduction was observed for all seasons. When considering all sites, the reduction was most pronounced in summer and autumn, but the general picture is that there is a minor seasonal variability in the reduction of EC. There are more sites with significant trends in summer than in winter (Table S18). These change in EC is consistent with the decreasing trends in equivalent black carbon (eBC) reported lately (Savadkoohi *et al.*, 2023). Several studies attribute reduced European EC levels to reduced vehicular emissions, following from effective mitigation policies such as introduction of particle filters (Borlaza *et al.*, 2022 and references therein).

The model captures the annual changes of EC very well over the ten years and captures well the relative changes, which are approximately $-4\% \text{ yr}^{-1}$ in all seasons. Larger differences between observations and model are seen in the absolute changes.

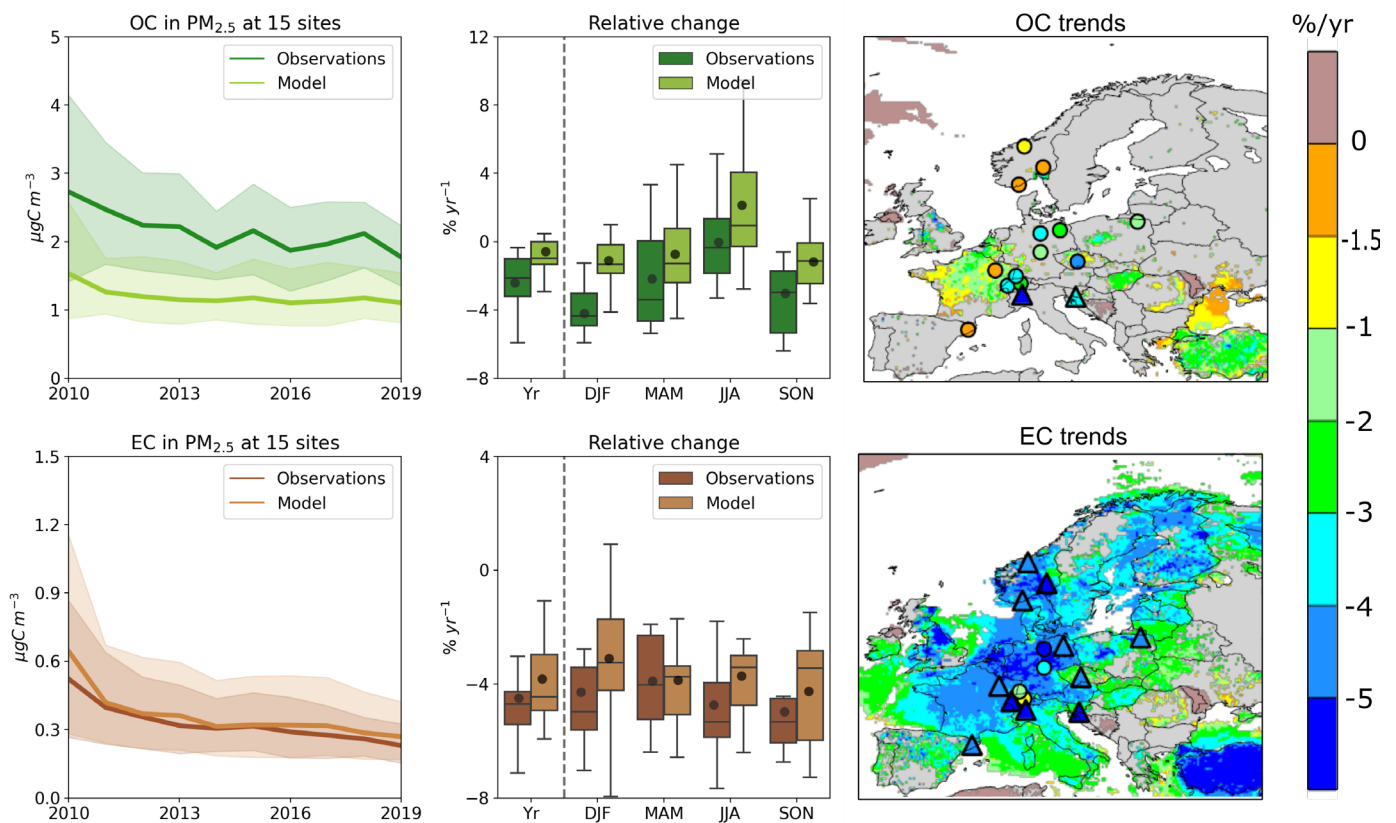
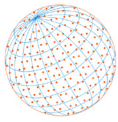
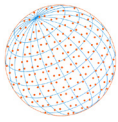


Fig. 3. Observed and modelled trends of OC and EC for 15 EMEP sites across Europe for 2010–2019 (left panels), aggregated annual relative changes (mid panels), and spatial relative trends (right panel). For explanation of what the shaded areas and map colours represent see Fig. 1 and Fig. 2.

A $2.4 \pm 1.6\% \text{ yr}^{-1}$ reduction in OC for 2010–2019 was calculated for the 15 sites assessed (Fig. 3). Statistically significant downward trends were only observed for Iskrba (Slovenia) and Ispra (Italy), which are amongst the sites with the highest OC loading. At these two sites, the reduction was noticeably higher ($-3.1\% \text{ yr}^{-1}$ at Iskrba; $-5.9\% \text{ yr}^{-1}$ at Ispra) than for the mean of all sites. The reduction in OC appears somewhat lower at the westernmost and northernmost sites (Fig. 3). There was a pronounced seasonal variability in the reduction observed for OC. In winter, the reduction ($-4.2\% \text{ yr}^{-1}$) was equal to that for EC ($-4.3\% \text{ yr}^{-1}$), but only statistically significant for six of the sites, whereas no reduction was seen in summer. Spring ($-2.2\% \text{ yr}^{-1}$) and autumn ($-3.0\% \text{ yr}^{-1}$) are transition seasons with reductions in between that of winter and summer and a statistically significant reduction was observed only for Ispra. The model substantially underpredicts the annual concentrations of OC over the whole period, as well as the trends. There is substantial seasonal variation though. Observed reductions in winter are not at all reproduced by the model ($-1.1\% \text{ yr}^{-1}$). In summer the model shows positive trends of $2.1\% \text{ yr}^{-1}$. Ten years is a short period to assess trends. To illustrate this, Table 1 shows trends assessed for three periods (2008–2018, 2008–2019, and 2010–2019) at Birkenes Observatory, using the same methodology. The results show that the magnitude of the trends can differ substantially depending on the time-window. For EC the values range from $-2.2\% \text{ yr}^{-1}$ to $-4.2\% \text{ yr}^{-1}$, and for levoglucosan from $-2.5\% \text{ yr}^{-1}$ to $-5.2\% \text{ yr}^{-1}$; all these trends are statistically significant. Trend values for OC vary even more than for EC and levoglucosan but were non-significant for all periods. Trends reflect changes both in emissions and in meteorological variation, the latter being most responsible for the high variability in the calculated trends for the different time windows.

The 2010–2019 reduction of $4.2\% \text{ yr}^{-1}$ in observed EC across all seasons is substantial, although different choices of time-windows (Table 1) suggest a less pronounced reduction. The lack of seasonal variability in the reduction of EC is puzzling since residential heating should have a clear

**Table 1.** Relative trends (% yr⁻¹) and *p*-values in parentheses calculated for Birkenes using different time-windows (2008–2018^(a) 2008–2019 2010–2019).

	2008–2018 ^(a)	2008–2019	2010–2019
EC	–3.00 (0.043)	–2.21 (0.034)	–4.24 (0.012)
OC	–0.44 (0.876)	0.18 (–) ^(b)	–0.64 (–)
Levoglucosan	–2.50 (0.043)	–2.48 (0.024)	–5.2 (0.032)

Notes: ^(a) Values for 2008–2018 use same procedure as for 2008–2019 and 2010–2019. Due to minor screening differences, numbers differ slightly from results of [Yttri et al. \(2021\)](#), which had 2008–2018 trends of –4.2% yr⁻¹ for EC and –2.8% yr⁻¹ for levoglucosan; ^(b) dash (–) indicates highly insignificant *p*-value.

winter maxima. [Yttri et al. \(2021\)](#) found that the reduction in EC was most pronounced in spring and summer at the Birkenes Observatory in southern Norway for 2001–2018, arguing that this was due to influence from less abated sources such as domestic heating in winter and autumn. This argument was supported by a smaller change (–2.8% yr⁻¹) for the biomass burning tracer levoglucosan (2008–2018) than for EC (–4.2% yr⁻¹). These trend numbers are from [Yttri et al. \(2021\)](#) and differ slightly from trends calculated for this report ([Table 1](#)). In the present study we calculated a yearly reduction of 5.2% yr⁻¹ for the biomass burning tracer levoglucosan observed at the Birkenes Observatory for 2010–2019. This is greater than the –4.2% yr⁻¹ change calculated for EC. Although it might seem contradictory to the findings of [Yttri et al. \(2021\)](#), it must be emphasized that the differences in trends result from using different time-windows, as shown in [Table 1](#). This underscores the challenges in reaching firm conclusions on trends for short time periods.

As the biomass burning emissions observed at the Birkenes Observatory are largely long-range transported from Continental Europe and Western Russia ([Yttri et al., 2021](#)), our findings for Birkenes are likely to be representative for a larger part of Europe. Variability in the source areas for the air masses arriving the Birkenes Observatory can influence the observed trends, but as the time-series is extended, these variations will be smoothed out, resulting in more reliable trend observations.

[Fig. 4](#) shows that for certain countries, such as France, PM_{2.5} emissions from residential heating have constantly decreased over the 2000s. Reductions in other countries from around 2010 mostly show a reduction of approximately 4% yr⁻¹. Thus, abatement of residential wood combustion (RWC) emissions seems to be progressing for many countries, though the magnitude of the contribution from different countries will vary from year to year.

Condensable organics impact estimates of PM_{2.5} emissions and their trends ([Denier van der Gon et al., 2015](#); [Simpson et al., 2020, 2022](#)), and [Fig. 4](#) illustrates this. French emissions include condensable organics in their reported PM emissions, whereas Germany does not ([Simpson et al., 2020](#)). This difference is a major reason for the magnitude of the French emissions from residential heating compared to those of the more highly populated Germany. We note that [Yttri et al. \(2021\)](#) found a statistically significant trend of similar magnitude and sign (–4.2% yr⁻¹) for EC for 2001–2018 as for 2010–2019 in the present study for the Birkenes Observatory. As this site has a footprint that covers a large part of continental Europe (*ibid.*), this consistency suggests a large-scale reduction in EC emissions over the last two decades. As discussed in [Simpson et al. \(2022\)](#), assumptions concerning the volatility of condensables, or addition of additional intermediate-volatility VOC, can also impact trend calculations of modelled data, but these refinements are very uncertain and beyond the scope of the present study.

Unlike EC, the observed seasonal trends for OC (c.f. [Fig. 3](#)) are very variable, with large (ca. 4%) reductions in the winter months (both DJF and SON), and apparently no change in summer. The lack of clear trends in summer is not surprising. Spring and especially summertime levels of OC are subject to substantial influences from natural sources, in particular from biogenic secondary organic aerosol (BSOA) and primary biological aerosol particles (PBAP) ([Gelencsér et al., 2007](#); [Yttri et al., 2021, 2019](#)). These biogenic emissions are not subject to abatement, but are very sensitive to meteorology, and thus summertime OC trends are strongly influenced by year-to-year changes in meteorological conditions. Anthropogenic OC emissions are likely best represented by wintertime

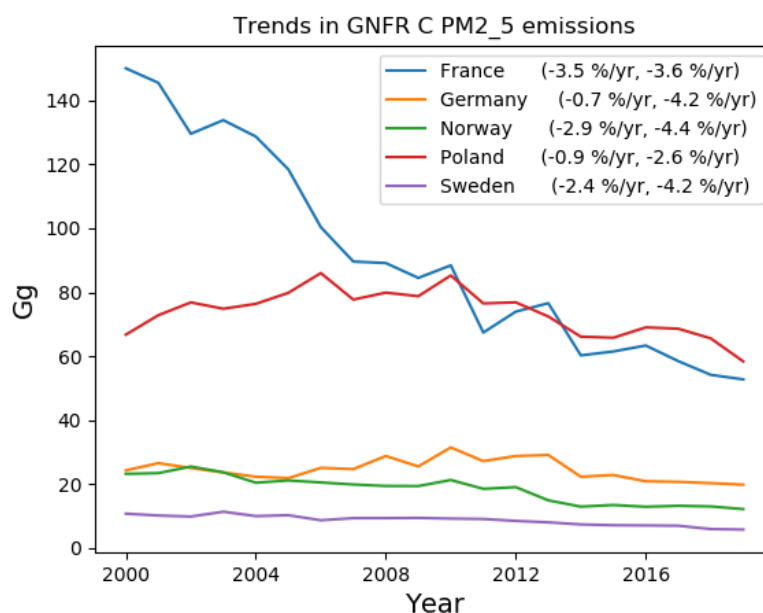
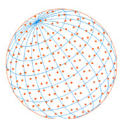


Fig. 4. Trends in PM_{2.5} emissions from the GNFR C (Gridded aggregated Nomenclature for Reporting from other stationary Combustion activities) emission sector which is mainly residential heating. Values in parentheses give relative trends (here linear regression slopes), for the periods 2000–2019 and 2010–2019.

data, and in DJF the observed trend of $-4\% \text{ yr}^{-1}$ for OC is rather similar to that found for EC. As for EC, domestic heating is an important source of OC all over Europe in the heating season (Yttri *et al.*, 2019), but especially where RWC is utilized (Gilardoni *et al.*, 2011). At the Birkenes Observatory, the wintertime reduction in OC ($-4.1\% \text{ yr}^{-1}$) was only somewhat lower than for EC ($-6.4\% \text{ yr}^{-1}$) and levoglucosan ($-4.6\% \text{ yr}^{-1}$). These results suggest that abatement of RWC emissions has been quite effective for Europe in general, taking into account the considerations made about the length of the time series and the Birkenes Observatory as an indicator of European emissions.

The underprediction of the wintertime OC levels should not be interpreted as a flaw in the EMEP model but is rather at least partly the result of the issues with missing condensable or intermediate-volatility organics. It has been demonstrated elsewhere that model results improve substantially when such compounds are included (Denier van der Gon *et al.*, 2015; Fagerli *et al.*, 2020; Robinson *et al.*, 2007; Simpson *et al.*, 2019, 2022). Inclusion of such compounds has been discussed in Simpson *et al.* (2020) but the necessary timeseries of emissions were not available for the current study.

3.4.1 OC and EC fractions of PM

The highest PM levels in Europe are often seen during winter periods with stagnant air and high emissions from RWC. The relative contribution of inorganic and carbonaceous matter to PM_{2.5} during the winter periods for 2000–2019 at four different sites is shown in Fig. 5. It highlights the importance of the organic fraction for a further reduction in wintertime PM_{2.5} mass concentration. As a first step, the natural and the anthropogenic fraction of the carbonaceous aerosol must be separated, then further separated into abatable categories. Separation of eBC into biomass burning (solid fuel) (eBC_{bb}) and fossil fuel (liquid fuel) (eBC_{ff}) is possible using data from the multi-wavelength aethalometer (Savadkoobi *et al.*, 2023; Platt *et al.*, 2020). Although not directly comparable to the multi-year plots presented in Fig. 5, results from the EMEP intensive measurement period during winter 2017/2018 (Platt *et al.*, 2020) illustrates the split between eBC_{bb} and eBC_{ff} for winter 2017/2018 at the respective sites, identifying biomass burning/solid fuel as the major source of eBC. The apportionment of eBC can also be used to infer the corresponding fractions of OM. An obvious next step is to implement such analysis as part of regular monitoring. This would enable validation of not just model performance, but also the

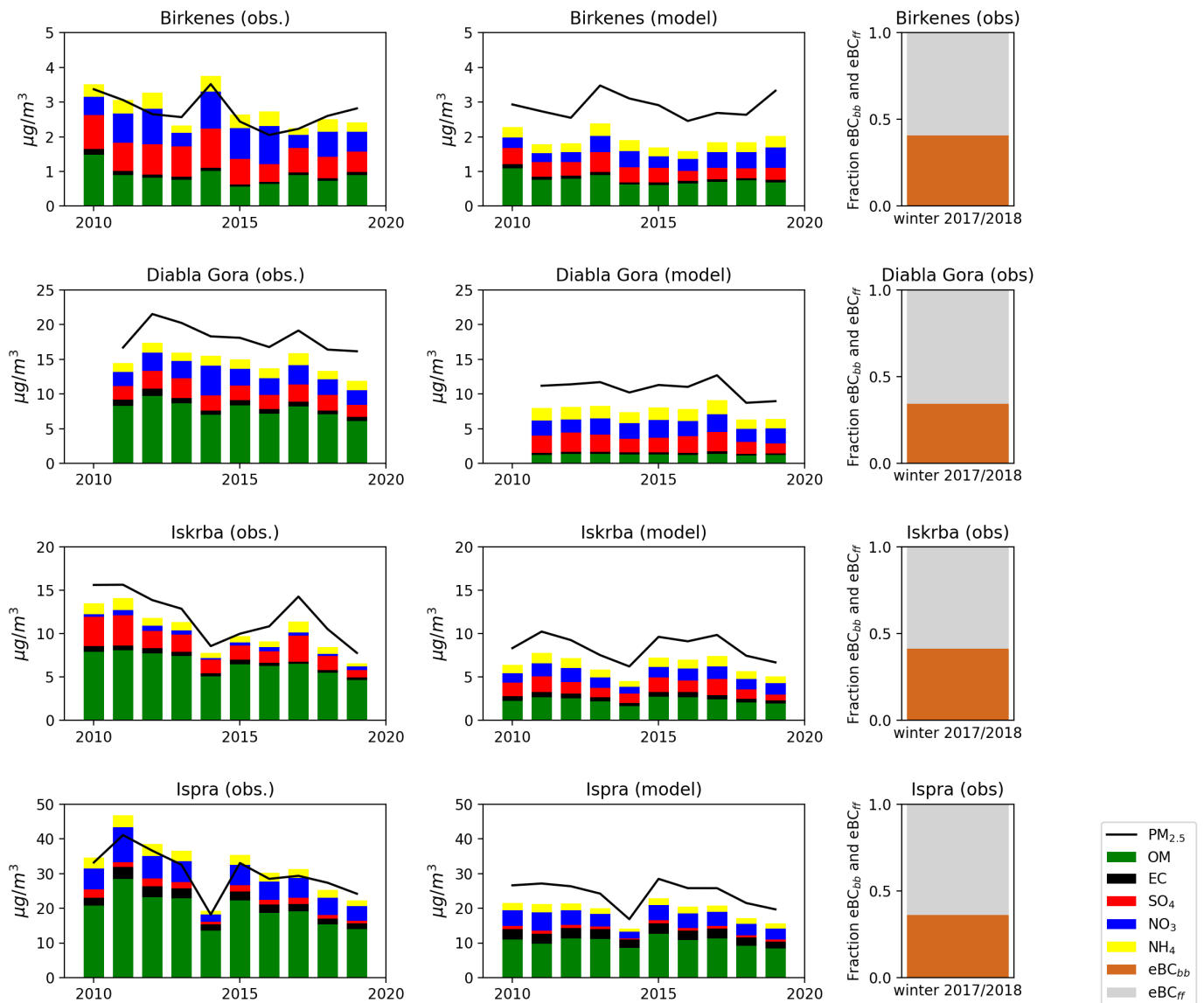
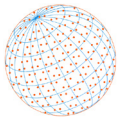


Fig. 5. Mass balance of wintertime $\text{PM}_{2.5}$ at Birkenes (NO002R), Diabla Gora (PL005R), Iskrba (SI008R), and Ispra (IT004R) including $\text{PM}_{2.5}$, organic mass (OM), EC, SO_4^{2-} , NO_3^- , NH_4^+ from observations (left), modelled (middle) and apportionment of eBC into biomass burning/solid fuel (eBC_{bb}) and fossil fuel/liquid fuel (eBC_{ff}) for winter 2017/2018 (right). Note that at Birkenes and Diabla Gora the SIA components in observations are from filterpack sampler with no cutoff and thus probably overestimate the $\text{PM}_{2.5}$ SIA. OM is calculated assuming $\text{OM} = \text{OC} \times 1.4$ for Ispra and 1.7 for the other sites).

effectiveness of initiatives aimed at reducing carbonaceous aerosol emissions from both fossil fuel and biomass burning sources.

3.5 Trends in PM_{10} and $\text{PM}_{2.5}$

The reduction of PM pollution is largely dependent on abatement strategies of anthropogenic gaseous precursor of secondary aerosols, as discussed above, though changes in primary PM emissions may also be important depending on site location. Annual timeseries of PM_{10} and $\text{PM}_{2.5}$ (Fig. 6, left panels) exhibit evident concentration reductions from 2000 to 2019, both for observational data and model simulations. In general, the model underestimates the concentrations, but reproduces quite well observed annual changes in both PM_{10} and $\text{PM}_{2.5}$. This includes enhanced PM levels due to meteorological conditions, such as for the dry and hot summer in 2003 (EMEP, 2005) and the dry conditions in 2011 in Western/Central/Southern Europe (EMEP, 2013). It should

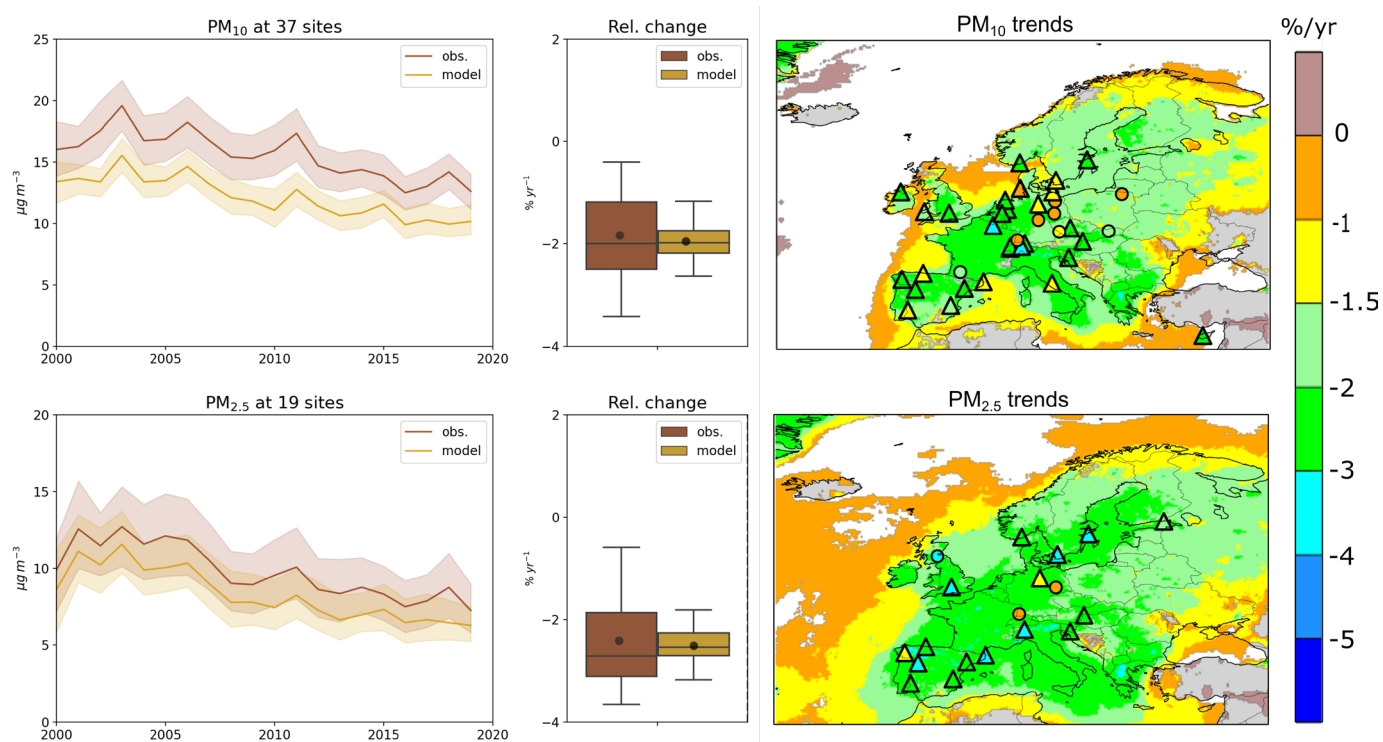
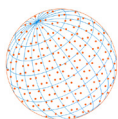


Fig. 6. Spatial and temporal trends in PM₁₀ and PM_{2.5} from 2000–2019. For explanation of what the shaded areas and map colours represent see Fig. 1 and Fig. 2.

be noted that the emission data used for the model runs does not include condensable organics consistently across countries, thus, part of the underestimation of PM can be related to this.

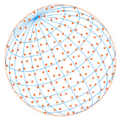
Statistically significant PM₁₀ and PM_{2.5} trends were identified for most of the sites (Fig. 6, right panels). For PM₁₀, the observed and model simulated relative reductions are on average $1.8 \pm 0.3\% \text{ yr}^{-1}$ and $2.0 \pm 0.2\% \text{ yr}^{-1}$ respectively, whilst reductions are on average $2.4\% \pm 0.4\% \text{ yr}^{-1}$ and $2.5\% \pm 0.2\% \text{ yr}^{-1}$ for PM_{2.5} (Tables S15 and S16), thus a total reduction of about 36% and 47% in PM₁₀ and PM_{2.5}, respectively.

The relative changes shown in Fig. 6 highlight a considerably greater variation in trends observed at different sites with respect to modelled trend, with the modelled trends falling within the inter-quartile range (IQR) (25–75%) of the observed ones.

The reductions of both primary PM emissions and those of PM precursor gases (SO_x, NO_x, NH₃, and VOCs) were drivers of the reductions in PM concentrations observed over the western part of the EMEP domain during the 2000–2019 period. Substantial reductions of SIA concentrations, and those of SO₄²⁻ in particular, made a crucial contribution to decreasing PM pollution, but also substantial reduction of emissions of primary PM₁₀ (by 32%) and PM_{2.5} (by 35%) contribute. OC, more than EC, accounts for a major fraction of (anthropogenic) primary PM_{2.5}, thus its contribution to the observed reduction in PM should not be overlooked. The major influence of natural emissions and the lack of (consistent) data covering the 20-year period studied makes it difficult to quantify the contribution made by OC.

3.6 Trends in O₃

Trend studies of surface ozone require a somewhat different approach than other species since ambient ozone levels are the result of a substantial baseline level with episodes of photochemical production or entrainment from aloft. Whereas NO_x often leads to ozone formation in rural areas in the summer season, it can cause depletion of ozone by titration in and downwind of urban areas, especially in winter. Thus, the effect of anthropogenic emissions of ozone precursors such as NO_x is to change the distribution of hourly and daily ozone concentrations during a year with increased ozone levels in summer and reduced ozone levels in winter. Furthermore, the extent



of these perturbations is significantly determined by the weather conditions and thereby by the ongoing climate change.

The selection of ozone metrics is decisive for the estimated trends (Lefohn *et al.*, 2018). The annual mean concentration used for evaluating other species is of little interest when studying ozone. A common procedure is to look at the trend in the probability distribution of ozone, e.g., by calculating trends for various percentiles of the distribution (Simpson *et al.*, 2014). Fig. 7 shows the calculated Sen's slopes for six percentiles (10, 50, 75, 95, 98, and 99) of the daily maximum O₃ values for the period 2000–2019 for EMEP sites north and south of 49°N. For both the observed and modelled data, the trends show an increase in the 10th percentile and with a gradually stronger decrease in the higher percentiles. This is as expected when the emission of precursors (NO_x) is reduced with time. The increase in the 10th percentile could be explained by reduced titration of NO_x, at least at sites exposed to surrounding emissions or long-range transport of NO_x. For remote sites, an increased level in the low percentiles could reflect changes in the hemispheric free-tropospheric baseline ozone. The decreasing trend in the highest percentiles is explained by reduced photochemical formation of ozone in summer. The net result of these trends is a narrowing of the distribution of O₃ concentrations. In general, the agreement between observations and model is rather good, with the model agreeing very well with the observations for the high percentiles for stations north of 49°N though overestimating somewhat the decrease of the high percentiles (95–99) for stations south of 49°N. This is an important finding since these percentiles are the main indicators for surface ozone pollution events. Fig. 7 furthermore shows that the spread in the observed data is significantly larger than the spread in modelled data which is as expected: A grid model will inevitably reduce local geographical differences and produce smoothed concentrations fields.

The modelled 10th and 50th percentiles are higher than the observations whereas the observed high percentiles (95–99) are higher than modelled. The bias in the high percentiles is particularly strong for stations south of 49°N.

The reason for the model to overestimate the 10th percentile is not obvious and one should note that these percentiles refer to the daily maximum values and not the hourly levels. Deficiencies in the modelled ozone diurnal cycle, particularly during periods of stable, stagnant winter situations could lead to discrepancies vs. the observed levels. It could also reflect that real NO_x concentrations in winter are not reduced as much as the emission inventories and the model assume, or it could e.g., reflect deficiencies in the model description of atmospheric vertical stability and exchange of pollutants in winter. A possible underprediction of European NO_x emissions was suggested as a likely cause of model underprediction of peak ozone and overprediction of low ozone by Oikonomakis *et al.* (2018). The interannual variation in the higher percentiles, i.e., the change in

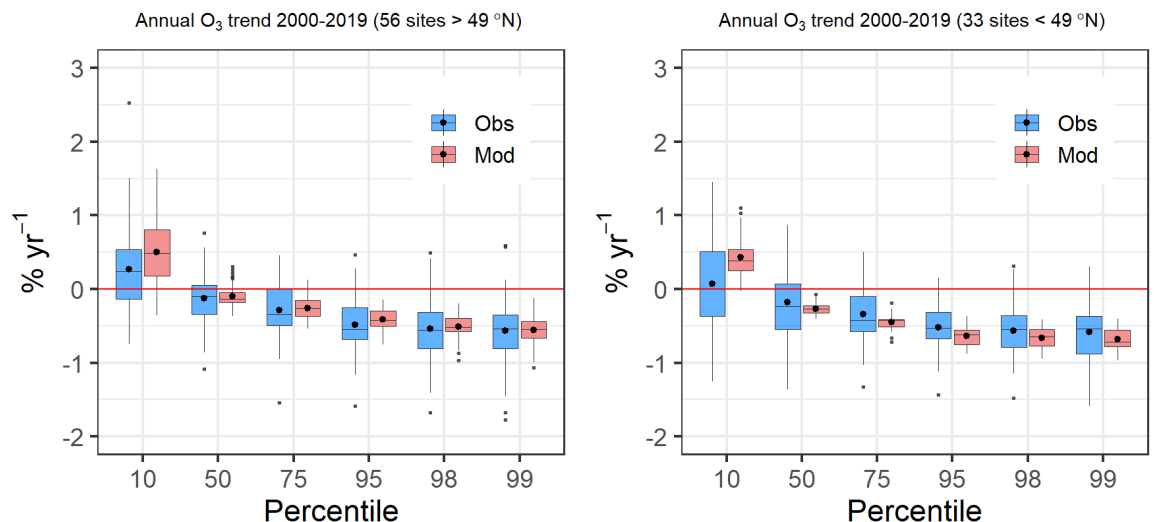


Fig. 7. Boxplot of trends in annual percentiles of daily max O₃ from 2000–2019 for EMEP observations and model calculations for stations north (left) and south (right) of 49°N. For explanation see Fig. 1.

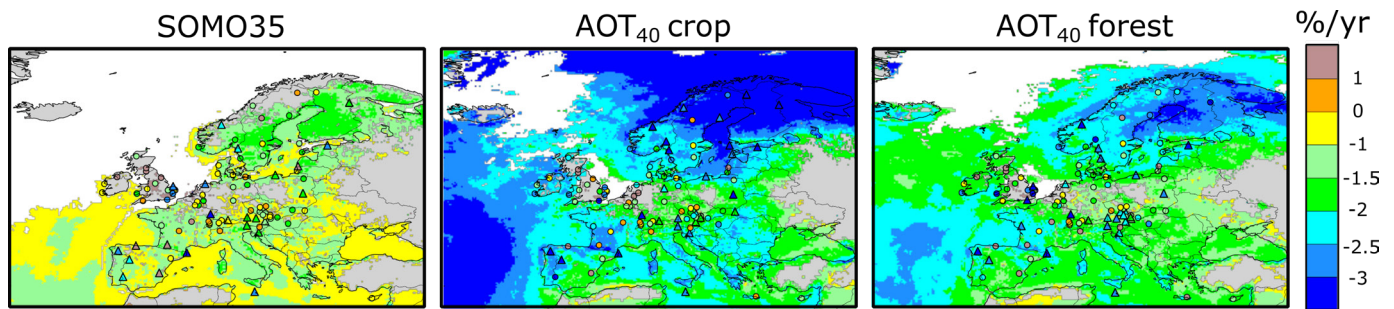
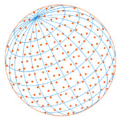


Fig. 8. Relative trends in different ozone effect metrics from 2000–2019. For explanation see Fig. 2.

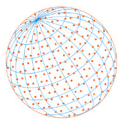
levels from year to year, is however very well reproduced by the model. Peak years as 2003 and 2006 in both regions as well as 2015 in the south and 2018 and 2019 in the north is reproduced by the model, the levels have however a substantial offset. This implies that the episodes leading to the peak values are captured by the model, but that the ozone levels during the episodes are underestimated.

Trends in ozone metrics linked to harmful effects on vegetation (AOT40 for crops and forest, here calculated from observations and modelled values at 3 m elevation) and on human health (SOMO35) are shown in Fig. 8. The absolute levels in AOT40 are underestimated by the model compared to the observed data (not shown). This might be because this metric is very sensitive to the hemispheric baseline O_3 concentration level (Sofiev and Tuovinen, 2001) which is close to the 35–40 ppb range. Thus, a small offset in the assumed model boundary conditions compared to the actual levels at the boundary could lead to substantial discrepancies. However, as shown in SI Fig. S6 in Etzold *et al.* (2020), the EMEP model can reproduce AOT40 quite well. For SOMO35 (Fig. 8), the model calculations agree very well with the observed data, both with respect to the absolute levels and the trends. Both the modelled and observed AOT40 and SOMO35 indicate declining levels during 2000–2019, but the fraction of significant trends is rather low, reflecting that these metrics are close to the background level and thereby sensitive to small fluctuations in the baseline ozone level. For all these metrics the model calculates stronger mean reductions than observed (Table S21).

4 CONCLUSIONS

Our trend study reveals significant improvements in Europe's environmental conditions over the past two decades. Notably, the reported European SO_x emissions have declined by over 80% since 2000, leading to substantial reductions in atmospheric sulfur components by 3–4% annually. The reported NO_x emissions have been reduced by almost 50%, resulting in a 1.5–2% annual reduction in oxidized nitrogen compounds in air and precipitation. Observed reductions of sulfur and oxidized nitrogen are somewhat smaller than model predictions, prompting the need for looking into reported emissions. Further investigations are needed to identify the sources of these differences. Ammonia emissions have seen limited reductions, but the concentration of particulate ammonium has notably decreased, due to reductions in SO_x and NO_x emissions.

Abatement measures have successfully reduced EC and OC levels over the last ten years, particularly during wintertime; trends in summertime OC were much less clear, almost certainly due to the impact of biogenic sources. Both PM_{10} and $PM_{2.5}$ concentrations exhibited significant downward trends, with $PM_{2.5}$ showing more substantial reductions, respectively about 1.9% and 2.5% annually. Ozone show significant reductions for the highest concentration levels, 0.3–0.6% annually. Also, the three aggregated effect metrics (AOT40 for crops, AOT40 for forests and SOMO35) show a decrease during the last two decades, 1–2% annually. Overall, our findings highlight positive environmental improvements in Europe, although some differences between observations and model predictions merit further investigation.



ACKNOWLEDGMENTS

The work presented was largely funded by EMEP under UN-ECE and was partly carried out as a contribution to the EMEP Task force of Measurement and modelling (TFMM). A large number of co-workers in participating countries have contributed in submitting quality assured data. The EMEP centres would like to express their gratitude for continued good co-operation and effort. The institutes and persons providing data are identified together with the data sets in the EBAS database. The program greatly benefits from its close ties to both The Aerosol, Clouds, and Trace Gases Research Infrastructure (ACTRIS) and the Global Atmosphere Watch (GAW) program under the World Meteorological Organization (WMO). These connections facilitate collaboration in sharing several of the Observatories and measurements, and in the development of quality assurance and quality control (QA/QC) procedures.

Computer time for EMEP model runs was supported by the Research Council of Norway through the NOTUR project EMEP (NN2890K) for CPU and the NorStore project European Monitoring and Evaluation Programme (NS9005K) for storage of data. The development of the EMEP MSC-W model has also been supported by the Nordic Council of Ministers, the Norwegian Space Centre and Environment and Copernicus Atmosphere Modelling Service (CAMS) projects. This study benefited from the Norwegian research council project 229796 (AeroCom-P3) especially for development of the `pyaerocom` tool. The Norwegian Ministry of Climate are also greatly acknowledged for supporting both model and database development at the EMEP Centres, MSC-W and CCC.

We also thank the reviewers and the editor for valuable contributions to the paper.

ADDITIONAL INFORMATION

Data Availability

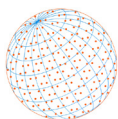
The observations collected at the EMEP monitoring network are annually reported to the Chemical Coordinating Centre of EMEP. All submitted observational data, after routine quality and consistency control, are available in EBAS (<https://ebas.nilu.no>). The scripts used for processing the data and calculating trends, are available from a GitHub repository (https://github.com/metno/emep_trends_2021). A trend interface showing the results for each individual site for the different periods and compounds has been developed and is available at https://aeroval.met.no/evaluation.php?project=emep-trends&exp_name=2000-2019&station=WORLD.

Supplementary Material

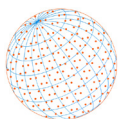
Supplementary material for this article can be found in the online version at <https://doi.org/10.4209/aaqr.230237>

REFERENCES

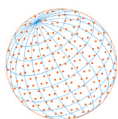
- Aas, W., Tsyro, S., Bieber, E., Bergström, R., Ceburnis, D., Ellermann, T., Fagerli, H., Frölich, M., Gehrig, R., Makkonen, U., Nemitz, E., Otjes, R., Perez, N., Perrino, C., Prévôt, A.S.H., Putaud, J.P., Simpson, D., Spindler, G., Vana, M., Yttri, K.E. (2012). Lessons learnt from the first EMEP intensive measurement periods. *Atmos. Chem. Phys.* 12, 8073–8094. <https://doi.org/10.5194/acp-12-8073-2012>
- Aas, W., Mortier, A., Bowersox, V., Cherian, R., Faluvegi, G., Fagerli, H., Hand, J., Klimont, Z., Galy-Lacaux, C., Lehmann, C.M.B., Myhre, C.L., Myhre, G., Olivieri, D., Sato, K., Quaas, J., Rao, P.S.P., Schulz, M., Shindell, D., Skeie, R.B., Stein, A., *et al.* (2019). Global and regional trends of atmospheric sulfur. *Sci. Rep.* 9, 953. <https://doi.org/10.1038/s41598-018-37304-0>
- Banzhaf, S., Schaap, M., Kranenburg, R., Manders, A.M.M., Segers, A.J., Visschedijk, A.J.H., Denier Van Der Gon, H.A.C., Kuenen, J.J.P., Van Meijgaard, E., Van Ulft, L.H., Cofala, J., Builtjes, P.J.H. (2015). Dynamic model evaluation for secondary inorganic aerosol and its precursors over Europe between 1990 and 2009. *Geosci. Model Dev.* 8, 1047–1070. <https://doi.org/10.5194/gmd-8-1047-2015>



- Borlaza, L.J., Weber, S., Marsal, A., Uzu, G., Jacob, V., Besombes, J.L., Chatain, M., Conil, S., Jaffrezo, J.L. (2022). Nine-year trends of PM₁₀ sources and oxidative potential in a rural background site in France. *Atmos. Chem. Phys.* 22, 8701–8723. <https://doi.org/10.5194/acp-22-8701-2022>
- Cavalli, F., Viana, M., Yttri, K.E., Genberg, J., Putaud, J.P. (2010). Toward a standardised thermal-optical protocol for measuring atmospheric organic and elemental carbon: the EUSAAR protocol. *Atmos. Meas. Tech.* 3, 79–89. <https://doi.org/10.5194/amt-3-79-2010>
- Colette, A., Aas, W., Banin, L., Braban, C.F., Ferm, M., González Ortiz, A., Ilyin, I., Mar, K., Pandolfi, M., Putaud, J.P., Shatalov, V., Solberg, S., Spindler, G., Tarasova, O., Vana, M., Adani, M., Almodovar, P., Berton, E., Bessagnet, B., Bohlin-Nizzetto, P., Boruvkova, J., Breivik, K., *et al.* (2016). Air pollution trends in the EMEP region between 1990 and 2012. Joint Report of the EMEP Task Force on Measurements and Modelling (TFMM), Chemical Co-ordinating Centre (CCC), Meteorological Synthesizing Centre-East (MSC-E), Meteorological Synthesizing Centre-West (MSC-W). EMEP/CCC-Report 1/2016, NILU, Kjeller, Norway.
- Colette, A., Solberg, S., Aas, W., Walker, S.E. (2021). Understanding Air Quality Trends in Europe, Focus on the relative contribution of changes in emission of activity sectors, natural fraction and meteorological variability. EIONET report ETC/ATNI 2020/8, NILU, Kjeller, Norway.
- Dalsøren, S.B., Myhre, C.L., Myhre, G., Gomez-Pelaez, A.J., Spøvde, O.A., Isaksen, I.S.A., Weiss, R.F., Harth, C.M. (2016). Atmospheric methane evolution the last 40 years. *Atmos. Chem. Phys.* 16, 3099–3126. <https://doi.org/10.5194/acp-16-3099-2016>
- Denier Van Der Gon, H.A.C., Bergström, R., Fountoukis, C., Johansson, C., Pandis, S.N., Simpson, D., Visschedijk, A.J.H. (2015). Particulate emissions from residential wood combustion in Europe – revised estimates and an evaluation. *Atmos. Chem. Phys.* 15, 6503–6519. <https://doi.org/10.5194/acp-15-6503-2015>
- Etzold, S., Ferretti, M., Reinds, G.J., Solberg, S., Gessler, A., Waldner, P., Schaub, M., Simpson, D., Benham, S., Hansen, K., Ingerslev, M., Jonard, M., Karlsson, P.E., Lindroos, A.J., Marchetto, A., Manninger, M., Meesenburg, H., Merilä, P., Nöjd, P., Rautio, P., *et al.* (2020). Nitrogen deposition is the most important environmental driver of growth of pure, even-aged and managed European forests. *For. Ecol. Manage.* 458, 117762. <https://doi.org/10.1016/j.foreco.2019.117762>
- European Monitoring and Evaluation Programme (EMEP) (2005). Transboundary Particulate Matter in Europe, EMEP Status report 4/2005. NILU, Kjeller, Norway.
- European Monitoring and Evaluation Programme (EMEP) (2013). Transboundary Particulate Matter in Europe. EMEP Status Report 4/2013. NILU, Kjeller, Norway.
- European Monitoring and Evaluation Programme (EMEP) (2021). Transboundary particulate matter, photo-oxidants, acidifying and eutrophying components, EMEP Status Report 2021, The Norwegian Meteorological Institute, Oslo, Norway.
- Fagerli, H., Aas, W. (2008). Trends of nitrogen in air and precipitation: Model results and observations at EMEP sites in Europe, 1980–2003. *Environ. Pollut.* 154, 448–461. <https://doi.org/10.1016/j.envpol.2008.01.024>
- Fagerli, H., Simpson, D., Wind, P., Tsyro, S., Nyíri, Á., Klein, H. (2020). Condensable organics; model evaluation and source receptor matrices for 2018, in: Transboundary particulate matter, photo-oxidants, acidifying and eutrophying components. EMEP Status Report 1/2020, pp. 83–97, The Norwegian Meteorological Institute, Oslo, Norway.
- Fowler, D., Pilegaard, K., Sutton, M.A., Ambus, P., Raivonen, M., Duyzer, J., Simpson, D., Fagerli, H., Fuzzi, S., Schjoerring, J.K., Granier, C., Neftel, A., Isaksen, I.S.A., Laj, P., Maione, M., Monks, P.S., Burkhardt, J., Daemmgen, U., Neiryneck, J., Personne, E., *et al.* (2009). Atmospheric composition change: Ecosystems–Atmosphere interactions. *Atmos. Environ.* 43, 5193–5267. <https://doi.org/10.1016/j.atmosenv.2009.07.068>
- Gelencsér, A., May, B., Simpson, D., Sánchez-Ochoa, A., Kasper-Giebl, A., Puxbaum, H., Caseiro, A., Pio, C., Legrand, M. (2007). Source apportionment of PM_{2.5} organic aerosol over Europe: Primary/secondary, natural/anthropogenic, and fossil/biogenic origin. *J. Geophys. Res.* 112, 2006JD008094. <https://doi.org/10.1029/2006JD008094>
- Gilardoni, S., Vignati, E., Cavalli, F., Putaud, J.P., Larsen, B.R., Karl, M., Stenström, K., Genberg, J., Henne, S., Dentener, F. (2011). Better constraints on sources of carbonaceous aerosols using a combined ¹⁴C – macro tracer analysis in a European rural background site. *Atmos. Chem.*

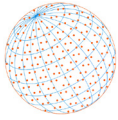


- Phys. 11, 5685–5700. <https://doi.org/10.5194/acp-11-5685-2011>
- Grange, S.K., Sintermann, J., Hueglin, C. (2023). Meteorologically normalised long-term trends of atmospheric ammonia (NH₃) in Switzerland/Liechtenstein and the explanatory role of gas-aerosol partitioning. *Sci. Total Environ.* 900, 165844. <https://doi.org/10.1016/j.scitotenv.2023.165844>
- Hamed, K.H., Ramachandra Rao, A. (1998). A modified Mann-Kendall trend test for autocorrelated data. *J. Hydrol.* 204, 182–196. [https://doi.org/10.1016/S0022-1694\(97\)00125-X](https://doi.org/10.1016/S0022-1694(97)00125-X)
- Hjellbrekke, A.G. (2021). Data Report 2019 Particulate matter, carbonaceous and inorganic compounds. EMEP/CCC Report 1/2021, NILU, Kjeller Norway.
- Hjellbrekke, A.G., Solberg, S. (2021). Ozone measurements 2019. EMEP/CCC Report 2/2021, NILU, Kjeller, Norway.
- Jiang, Z., Zhu, R., Miyazaki, K., McDonald, B.C., Klimont, Z., Zheng, B., Boersma, K.F., Zhang, Q., Worden, H., Worden, J.R., Henze, D.K., Jones, D.B.A., Denier Van Der Gon, H.A.C., Eskes, H. (2022). Decadal variabilities in tropospheric nitrogen oxides over United States, Europe, and China. *J. Geophys. Res.* 127, e2021JD035872. <https://doi.org/10.1029/2021JD035872>
- Jonson, J.E., Simpson, D., Fagerli, H., Solberg, S. (2006). Can we explain the trends in European ozone levels? *Atmos. Chem. Phys.* 6, 51–66. <https://doi.org/10.5194/acp-6-51-2006>
- Klimont, Z., Kupiainen, K., Heyes, C., Purohit, P., Cofala, J., Rafaj, P., Borken-Kleefeld, J., Schöpp, W. (2017). Global anthropogenic emissions of particulate matter including black carbon. *Atmos. Chem. Phys.* 17, 8681–8723. <https://doi.org/10.5194/acp-17-8681-2017>
- Lefohn, A.S., Malley, C.S., Smith, L., Wells, B., Hazucha, M., Simon, H., Naik, V., Mills, G., Schultz, M.G., Paoletti, E., De Marco, A., Xu, X., Zhang, L., Wang, T., Neufeld, H.S., Musselman, R.C., Tarasick, D., Brauer, M., Feng, Z., Tang, H., *et al.* (2018). Tropospheric ozone assessment report: Global ozone metrics for climate change, human health, and crop/ecosystem research. *Elem. Sci. Anth.* 6, 27. <https://doi.org/10.1525/elementa.279>
- Mortier, A., Gliš, J., Schulz, M., Aas, W., Andrews, E., Bian, H., Chin, M., Ginoux, P., Hand, J., Holben, B., Zhang, H., Kipling, Z., Kirkevåg, A., Laj, P., Lurton, T., Myhre, G., Neubauer, D., Olivie, D., Von Salzen, K., Skeie, R.B., *et al.* (2020). Evaluation of climate model aerosol trends with ground-based observations over the last 2 decades – an AeroCom and CMIP6 analysis. *Atmos. Chem. Phys.* 20, 13355–13378. <https://doi.org/10.5194/acp-20-13355-2020>
- Oikonomakis, E., Aksoyoglu, S., Ciarelli, G., Baltensperger, U., Prévôt, A.S.H. (2018). Low modeled ozone production suggests underestimation of precursor emissions (especially NO_x) in Europe. *Atmos. Chem. Phys.* 18, 2175–2198. <https://doi.org/10.5194/acp-18-2175-2018>
- Platt, S.M., Yttri, K.E., Aas, W. (2020). The winter 2017/2018 intensive measurement period. A brief update. In: *Transboundary particulate matter, photo-oxidants, acidifying and eutrophying components*, EMEP Status Report 1/2020, 145-152, The Norwegian Meteorological Institute, Oslo, Norway.
- Redington, A.L., Derwent, R.G., Witham, C.S., Manning, A.J. (2009). Sensitivity of modelled sulphate and nitrate aerosol to cloud, pH and ammonia emissions. *Atmos. Environ.* 43, 3227–3234. <https://doi.org/10.1016/j.atmosenv.2009.03.041>
- Robinson, A.L., Donahue, N.M., Shrivastava, M.K., Weitkamp, E.A., Sage, A.M., Grieshop, A.P., Lane, T.E., Pierce, J.R., Pandis, S.N. (2007). Rethinking organic aerosols: Semivolatile emissions and photochemical aging. *Science* 315, 1259–1262. <https://doi.org/10.1126/science.1133061>
- Savadkoobi, M., Pandolfi, M., Reche, C., Niemi, J.V., Mooibroek, D., Titos, G., Green, D.C., Tremper, A.H., Hueglin, C., Liakakou, E., Mihalopoulos, N., Stavroulas, I., Artiñano, B., Coz, E., Alados-Arboledas, L., Beddows, D., Riffault, V., De Brito, J.F., Bastian, S., Baudic, A., *et al.* (2023). The variability of mass concentrations and source apportionment analysis of equivalent black carbon across urban Europe. *Environ. Int.* 178, 108081. <https://doi.org/10.1016/j.envint.2023.108081>
- Sen, P.K. (1968). Estimates of the regression coefficient based on Kendall's Tau. *J. Am. Stat. Assoc.* 63, 1379–1389. <https://doi.org/10.1080/01621459.1968.10480934>
- Simpson, D., Benedictow, A., Berge, H., Bergström, R., Emberson, L.D., Fagerli, H., Flechard, C.R., Hayman, G.D., Gauss, M., Jonson, J.E., Jenkin, M.E., Nyíri, A., Richter, C., Semeena, V.S., Tsyro, S., Tuovinen, J.P., Valdebenito, Á., Wind, P. (2012). The EMEP MSC-W chemical transport model – technical description. *Atmos. Chem. Phys.* 12, 7825–7865. <https://doi.org/10.5194/acp-12-7825-2012>



7825-2012

- Simpson, D., Arneth, A., Mills, G., Solberg, S., Uddling, J. (2014). Ozone — the persistent menace: interactions with the N cycle and climate change. *Curr. Opin. Environ. Sustain.* 9–10, 9–19. <https://doi.org/10.1016/j.cosust.2014.07.008>
- Simpson, D., Bergström, R., Denier van der Gon, H., Kuenen, J.P., Schindlbacher, S., Visschedijk, A.J.H. (2019). Condensable organics; issues and implications for EMEP calculations and source-receptor matrices. Chapter 5 in EMEP Status Report 1/2021, pp. 71–88, Norwegian Meteorological Institute, Oslo, Norway.
- Simpson, D., Fagerli, H., Colette, A., van der Gon, H.D., Dore, C., Hallquist, M., Hansson, H., Maas, R., Rouil, L., Allemand, N. (2020). How should condensables be included in PM emission inventories reported to EMEP/CLRTAP? Report of the expert workshop on condensable organics organised by MSC-W, Gothenburg, 17-19th March 2020, EMEP Technical Report MSC-W 4/2020. https://emep.int/publ/reports/2020/emep_mscw_technical_report_4_2020.pdf
- Simpson, D., Gauss, M., Mu, Q., Tsyro, S., Valdebenito, A., Wind, P. (2021). Updates to the EMEP/MSW model, 2020–2021, in: Transboundary particulate matter, photo-oxidants, acidifying and eutrophying components. EMEP Status Report 1/2021, The Norwegian Meteorological Institute, Oslo, Norway, 109–12 Oslo, Norway.
- Simpson, D., Kuenen, J., Fagerli, H., Heinesen, D., Benedictow, A., Denier Van Der Gon, H., Visschedijk, A., Klimont, Z., Aas, W., Lin, Y., Yttri, K.E., Paunu, V.V. (2022). Revising PM_{2.5} emissions from residential combustion, 2005–2019. Nordic Council of Ministers, Denmark. <https://doi.org/10.6027/temanord2022-540>
- Sofiev, M., Tuovinen, J.P. (2001). Factors determining the robustness of AOT40 and other ozone exposure indices. *Atmos. Environ.* 35, 3521–3528. [https://doi.org/10.1016/S1352-2310\(01\)00086-3](https://doi.org/10.1016/S1352-2310(01)00086-3)
- Theobald, M.R., Vivanco, M.G., Aas, W., Andersson, C., Ciarelli, G., Couvidat, F., Cuvelier, K., Manders, A., Mircea, M., Pay, M.T., Tsyro, S., Adani, M., Bergström, R., Bessagnet, B., Briganti, G., Cappelletti, A., D'Isidoro, M., Fagerli, H., Mar, K., Otero, N., *et al.* (2019). An evaluation of European nitrogen and sulfur wet deposition and their trends estimated by six chemistry transport models for the period 1990–2010. *Atmos. Chem. Phys.* 19, 379–405. <https://doi.org/10.5194/acp-19-379-2019>
- Tørseth, K., Aas, W., Breivik, K., Fjæraa, A.M., Fiebig, M., Hjellbrekke, A.G., Lund Myhre, C., Solberg, S., Yttri, K.E. (2012). Introduction to the European Monitoring and Evaluation Programme (EMEP) and observed atmospheric composition change during 1972–2009. *Atmos. Chem. Phys.* 12, 5447–5481. <https://doi.org/10.5194/acp-12-5447-2012>
- Tsyro, S., Aas, W., Colette, A., Andersson, C., Bessagnet, B., Ciarelli, G., Couvidat, F., Cuvelier, K., Manders, A., Mar, K., Mircea, M., Otero, N., Pay, M.T., Raffort, V., Roustan, Y., Theobald, M.R., Vivanco, M.G., Fagerli, H., Wind, P., Briganti, G., *et al.* (2022). Eurodelta multi-model simulated and observed particulate matter trends in Europe in the period of 1990–2010. *Atmos. Chem. Phys.* 22, 7207–7257. <https://doi.org/10.5194/acp-22-7207-2022>
- United Nations Economic Commission for Europe (UNECE) (2012). Adjustments under the Gothenburg Protocol to emission reduction commitments or to inventories for the purposes of comparing total national emissions with them. Decision 2012/3, ECE/EB.AIR/113/Add.1. https://unece.org/fileadmin/DAM/env/documents/2013/air/ECE_EB.AIR_111_Add.1_ENG_DECISION_3.pdf
- Vaughan, A.R., Lee, J.D., Misztal, P.K., Metzger, S., Shaw, M.D., Lewis, A.C., Purvis, R.M., Carslaw, D.C., Goldstein, A.H., Hewitt, C.N., Davison, B., Beevers, S.D., Karl, T.G. (2016). Spatially resolved flux measurements of NO_x from London suggest significantly higher emissions than predicted by inventories. *Faraday Discuss.* 189, 455–472. <https://doi.org/10.1039/C5FD00170F>
- Vivanco, M.G., Theobald, M.R., García-Gómez, H., Garrido, J.L., Prank, M., Aas, W., Adani, M., Alyuz, U., Andersson, C., Bellasio, R., Bessagnet, B., Bianconi, R., Bieser, J., Brandt, J., Briganti, G., Cappelletti, A., Curci, G., Christensen, J.H., Colette, A., Couvidat, F., *et al.* (2018). Modeled deposition of nitrogen and sulfur in Europe estimated by 14 air quality model systems: evaluation, effects of changes in emissions and implications for habitat protection. *Atmos. Chem. Phys.* 18, 10199–10218. <https://doi.org/10.5194/acp-18-10199-2018>
- Yttri, K.E., Simpson, D., Bergström, R., Kiss, G., Szidat, S., Ceburnis, D., Eckhardt, S., Hueglin, C.,



- Nøjgaard, J.K., Perrino, C., Pizzo, I., Prevot, A.S.H., Putaud, J.P., Spindler, G., Vana, M., Zhang, Y.L., Aas, W. (2019). The EMEP Intensive Measurement Period campaign, 2008–2009: characterizing carbonaceous aerosol at nine rural sites in Europe. *Atmos. Chem. Phys.* 19, 4211–4233. <https://doi.org/10.5194/acp-19-4211-2019>
- Yttri, K.E., Canonaco, F., Eckhardt, S., Evangeliou, N., Fiebig, M., Gundersen, H., Hjellbrekke, A.G., Lund Myhre, C., Platt, S.M., Prévôt, A.S.H., Simpson, D., Solberg, S., Surratt, J., Tørseth, K., Uggerud, H., Vadset, M., Wan, X., Aas, W. (2021). Trends, composition, and sources of carbonaceous aerosol at the Birkenes Observatory, northern Europe, 2001–2018. *Atmos. Chem. Phys.* 21, 7149–7170. <https://doi.org/10.5194/acp-21-7149-2021>